

# Electron density shift description of non-bonding intramolecular interactions

Goar Sánchez-Sanz<sup>a,\*</sup>, Cristina Trujillo<sup>a,b</sup>, Ibon Alkorta<sup>a</sup>, José Elguero<sup>a</sup>

<sup>a</sup> Instituto de Química Médica, CSIC, Juan de la Cierva, 3, E-28006 Madrid, Spain

<sup>b</sup> Departamento de Ciencia e Ingeniería de Materiales e Ingeniería Química, Universidad Carlos III, Avda. de la Universidad 30, E-28911 Leganés, Madrid, Spain

## ARTICLE INFO

### Article history:

Received 14 March 2012

Received in revised form 9 April 2012

Accepted 10 April 2012

Available online 14 April 2012

### Keywords:

MP2

Intramolecular interactions

Electron density shift

Molecular tailoring

## ABSTRACT

A new methodology is described for the study of the electron density shift in intramolecular interactions. The methodology has been tested in an intermolecular complex and compared to the electron density shift obtained as the difference between the complex and the isolated monomers. The molecular fragmentation procedures and its application to hydrogen bonds, chalcogen–chalcogen interactions, nitrogen–boron interactions, dihydrogen interactions and silicon–nitrogen interactions are described. A careful selection of the fragmentation scheme is necessary in order to describe correctly the electron density shift in the intramolecular interactions. For this reason, different orders of fragmentation have been studied and analyzed pointing out the problems and limitations which are inherent to the methodology. It has been found that this methodology is a new tool which provides a good qualitative description of the electron density shift within the interacting region between two or more contacts, in both inter and intramolecular contacts with a reasonable low computational cost.

© 2012 Elsevier B.V. All rights reserved.

## 1. Introduction

Non-covalent interactions are the subject of many studies, some of them very recent. The reason is that they are present in almost every biological system, from small and simple molecules as H<sub>2</sub>O [1–4] to large and complex systems as DNA [5,6], from gas phase, liquids and even in solids those interactions play an important role in the structure of matter [7]. The number of non-covalent interactions is quite large, including hydrogen bonds [8–10], halogen bonds [11], ion- $\pi$  [12,13], pnictogens [14,15], chalcogens [16,17], stacking [18–20], and several others.

These interactions can be classified according to the systems in which they occur as inter- or intra-molecular interactions. As in other partition schemes, the intermolecular case is much simpler than the intramolecular one. For this reason, intermolecular interactions have been extensively studied with different approaches like supramolecular [21,22], and SAPT methodologies [23,24]. The intramolecular interactions have been much less studied due to the difficulties in their description [25]. Nevertheless, the importance of intramolecular hydrogen bonding in medicinal chemistry has been recently stressed [26].

In order to obtain a description of the intramolecular interaction, one has to separate the interacting part from the rest of the molecule. This is a problem which can be approached by the fragmentation of the system in smaller interacting parts. In Fig. 1 we have schematized the inter- and intra-molecular situations: in

the first one a non-covalent interaction should be broken while in the second one, a covalent bond has to be broken. However, if we consider that all bonds, covalent and non-covalent, share some common properties, *i.e.* that there is a continuum [27,28], then we could consider a third possibility when both bonds will be broken (new model).

In order to face the molecular scaling problem, some approaches based on molecular fragmentation have been proposed [29,30], in which different approximations are used to describe the molecular energy through the interaction energies between individual molecular fragments. The molecular tailoring approach proposed by Deshmukh et al. [31,32] allows the estimation of the hydrogen bond energies in polyhydroxy compounds and polypeptides [33].

Among all techniques that provide information of the interaction between two different systems, the study of the electron density is one of the most useful, and provides an ideal tool to understand these interactions [34–36]. The study of the electron density in molecules has been in the scope of the scientific community for several decades. Different approaches have been proposed to describe the electron density and its bonding properties [37]. The analysis of the electron transfer within the formation of the complexes as the difference between the electron density of the complex and the isolated monomers provides information in order to characterize these interactions [38–40]. In fact, the electron density shift has been used to analyze the non-bonding intermolecular interactions for different types of complexes as hydrogen bonds [40,41], pnictogen interactions [15,42],  $\pi$ -halogen interactions [43], halogen–hydride interactions [44] and other non-covalent interactions [45,46].

\* Corresponding author.

E-mail address: [goar@iqm.csic.es](mailto:goar@iqm.csic.es) (G. Sánchez-Sanz).

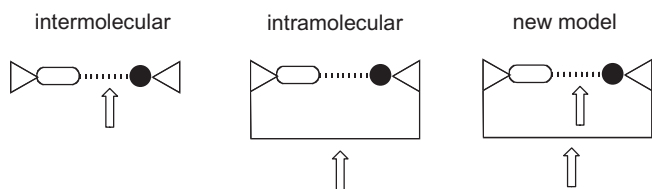


**Fig. 1.** Three different situations for interactions (the arrows point to the bonds that have to be broken to characterize the interaction).

The main aim of this article is to describe a fragment based method to estimate the electron density shift (EDS) within intermolecular and intramolecular interactions. With this objective in mind, it is very important to perform a partition of the molecule that allows representing properly the electron density shift between the interacting groups.

## 2. Computational details

All geometries were fully optimized at MP2 computational level [47]. We have used Dunning basis set, aug-cc-pVTZ [48,49] for the heteroatoms (O, Cl, F, N, B), cc-pVDZ for C, and H and pseudopotential LANL2DZ for Te in order to have a good compromise between accuracy and low computational cost. All the calculations have been carried out using the Gaussian-09 program [50]. The topological analysis of the electron density within the atoms in molecules (AIM) methodology [34] has been used to characterize the interactions. For this purpose, the AIMAll program has been used [51].

In order to have a quantitative measurement of the similarity of the electron density shifts (EDSs) generated, for the same system in different ways, the Hodgkin similarity index [52] has been used. Based in this index ( $H_{XY}$ ), the similarity of two EDSs,  $X$  and  $Y$ , is calculated as expressed by the following equation:

$$H_{XY} = \frac{2 \sum_{i=1}^A \text{EDS}(X)_i \text{EDS}(Y)_i}{\sqrt{\sum_{i=1}^A \text{EDS}(X)_i^2} \sqrt{\sum_{i=1}^A \text{EDS}(Y)_i^2}} \quad (1)$$

where  $\text{EDS}(N)$  ( $N = X$  or  $Y$ ) is the value for the EDS for each molecule at the same point ( $i$ ) of the three-dimensional grid with  $A$  points generated for the same system with two different methods. The maximum value of this index is 1, indicating that both electron densities are identical. It should be noted that the original definition of the Hodgkin index was computed analytically [in Eq. (1) the summation symbols should be changed to integral symbols]. However, in this work all the indexes have been computed numerically. This is for practical reasons, to allow straightforward computation of the molecular properties on a cubic grid and the generation of the three-dimensional maps.

The EDS are constructed using a 3D rectangular grid of approximately  $10^6$  points in the three directions of the space, in which the molecule is located in the center of the grid and the limit of the generated cube are 5 Å larger than the dimensions on the molecule. The quality of this grid has been checked in some test cases using a denser grid of  $8 \times 10^6$ , obtaining identical results.

The effect of the BSSE correction on the EDS has been explored using the same basis set for all the fragments of a given systems, 1,4-butanediol. The results obtained are identical considering or not the BSSE correction.

## 3. Methodology

The main aim of the present work is to describe a new tool which allows representing the electron density shift in those regions where non-bonding interactions are expected. The

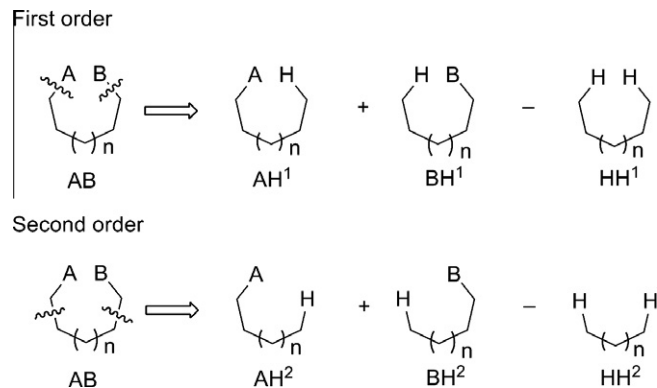


**Fig. 2.** Schematic representation of first and second order fragmentation in a generic system.

methodology can be applied to both inter and intramolecular interactions. However, since the evaluation of the intermolecular electron density shift can be easily obtained by subtracting the total electron density of the system and the sum of the isolated molecules that form it, we consider that the methodology described here is more suitable for intramolecular interactions.

The first step of the procedure corresponds to the fragmentation of the system of interest in different subsystems. In this case, we will consider that the fragmentation of the system will be carried out at the same bond distance of the interacting moieties,  $A$  and  $B$ . The fragments will maintain the geometry of the original system, except for the addition of hydrogen caps at fixed distances and maintaining the orientation of the bond broken.

Depending on the bond distances between the broken bond and the interacting moieties, the fragmentation order will be defined. First order fragmentation corresponds to the case where the bond broken is the one connecting the interacting moieties with the rest of the system (Fig. 2). Second order fragmentation is when two bonds separate the interacting moieties and the rest of the system and so on. In each case, three fragments are generated named as  $AH^n$ ,  $BH^n$  and  $HH^n$ . The superscript  $n$  represents the order of the fragmentation and  $AH^n$  and  $BH^n$  correspond to the fragments without  $B$  and  $A$  moieties, respectively and  $HH^n$  the one without  $A$  and  $B$  simultaneously.

The electron density shift of fragmentation order  $n$  due to the interaction of the  $A$  and  $B$  moieties can be calculated using the following equation:

$$\text{EDS}^n = \rho_{AB} - \rho_{AH}^n - \rho_{BH}^n + \rho_{HH}^n \quad (2)$$

where  $\rho_{AB}$ ,  $\rho_{AH}^n$ ,  $\rho_{BH}^n$  and  $\rho_{HH}^n$  are the electron densities of the whole system,  $AH$ ,  $BH$  and  $HH$  fragments using the fragmentation of  $n$  order, respectively.

## 4. Results and discussion

### 4.1. Intermolecular interactions

As a test of the methodology proposed, the EDS in an intermolecular complex using the procedure described before has been compared to the one calculated directly from the subtraction of the total electron density from the sum of the isolated molecules. In order to do that, the system chosen has been a dimer of  $n$ -propanol due to (a) it allows calculating the intermolecular EDS, (b) if we consider it as a whole linked system the intramolecular EDS can be calculated up to the third order of fragmentation, (c) both inter- and intra-molecular EDS can be compared.

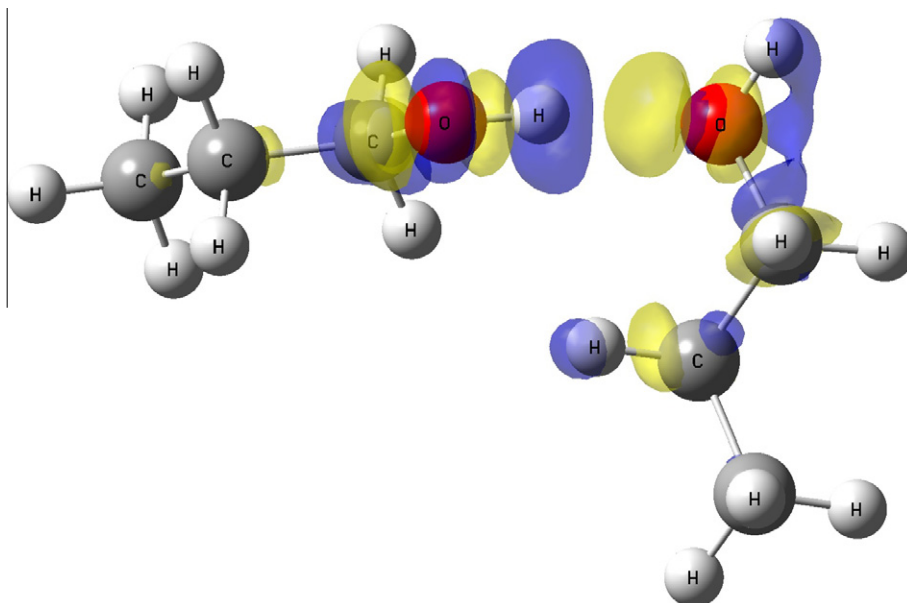


**Fig. 3.** Intermolecular EDS ( $\pm 0.001$  a.u. isosurfaces) for the dimer of propanol calculated as the difference of the electron density of the dimer minus the sum of the isolated monomers within the conformation of the dimer at MP2/aug-cc-pVTZ level computational level. Blue and yellow regions correspond to negative and positive values of the electron density shift, respectively.

In Fig. 3, the intermolecular EDS is shown. The HB donor and acceptor density shift pattern is shown for the intermolecular dimer. On one hand, a blue<sup>1</sup> region is observed surrounding the hydrogen corresponding to the HB donor, which represents a decrease of the electron density on this area. On the other hand, there is an increase in the intermolecular density on the zone located between that hydrogen atom and the oxygen one which act as a HB acceptor. This increase on the density is shown as a positive yellow region. The remaining blue and yellow areas in the molecules stress the transmitted effect of the HB along the carbon backbone. In Fig. 4, the EDS for the same system using the fragmentation scheme previously indicated is presented.

The comparison between Figs. 3 and 4 indicate that the first order EDS provides a good estimation of the variation of the electron density in the region containing the three atoms involved in the hydrogen bond interaction (OH $\cdots$ O). The calculated Hodgkin similarity index between the EDS shown in Fig. 3 and those of the first order fragmentation show value of 0.926.

The second order EDS provides not only a good description of the variation in the interaction area but in the bonds attached to the interacting moieties. In fact, as the order of the fragmentation increases, the better is the description of the EDS. These results are corroborated by the values of the similarity indexes which are 0.980 for the second order fragmentation EDS and 0.998 for the third order one.

In practice, the fragmentation order does not affect significantly the description of the intramolecular EDS within the area located between the interacting moieties. Nevertheless, if one wants to obtain the most accurate EDS, the higher order fragmentations are recommended.

Finally, in order to extend the methodology to larger systems, it has been checked the results obtained with a smaller basis set. Thus, the aug-cc-pVTZ basis set has been used for the oxygen atoms while the rest of the atoms (C and Hs) have been described with the cc-pVDZ (this basis set will be named as aug'-cc-pVTZ from now in the present article). The similarity indexes between

the EDS calculated at the MP2/aug-cc-pVTZ and MP2/aug'-cc-pVTZ for the three fragmentation orders considered in this system are between 0.997 and 0.998. These results indicate that both basis sets provide very similar results.

## 4.2. Intramolecular interactions

### 4.2.1. Case 1: 1,4-butanediol

In order to check the performance of the methodology described before to study EDS in intramolecular interactions, a relatively simple system, 1,4-butanediol, has been chosen. The most stable configuration of this molecule presents an OH $\cdots$ O hydrogen bond, as described by Jesus et al. [53] at MP2/6-311++G(d,p) computational level.

The analysis of the electron density of the mentioned conformer optimized at the MP2/aug'-cc-pVTZ computational level shows the presence of a bond critical point (BCP) which can be associated to an intramolecular HB. The interatomic distance between the two atoms involved (oxygen and hydrogen) is 1.833 Å and the value of the electron density at the BCP is 0.034 a.u.

In Fig. 5, left, the intramolecular electron density shift corresponding to the first fragmentation order is represented. It is interesting to notice that a similar pattern to the one shown in the inter- and intra-molecular EDS of the dimer of *n*-propanol (Figs. 3 and 4) is observed. Thus, the map indicates a reduction of the electron density around the hydrogen atom of the HB donor and an increment in the interatomic region closed to the hydrogen bond acceptor oxygen atom.

In the second order fragmentation EDS, Fig. 5, right, it can be observed that the electron variation is extended in the molecular framework in closed similarity to what is observed in the *n*-propanol dimer already described. The value of the Hodgkin similarity index between the first and second order fragmentation EDS of the intramolecular interaction of the 1,4-butanediol is 0.928.

The fragmentation pattern proposed here presents some limitations. Thus, if the third order fragmentation (Fig. 6) is applied to the 1,4-butanediol molecule, the HH<sup>3</sup> fragment corresponds to the H<sub>2</sub> molecule. This drives to a spurious EDS between C2 and C3 where the system is fragmented twice. This is because the

<sup>1</sup> For interpretation of color in Figs. 3–9, 11–13, the reader is referred to the web version of this article.

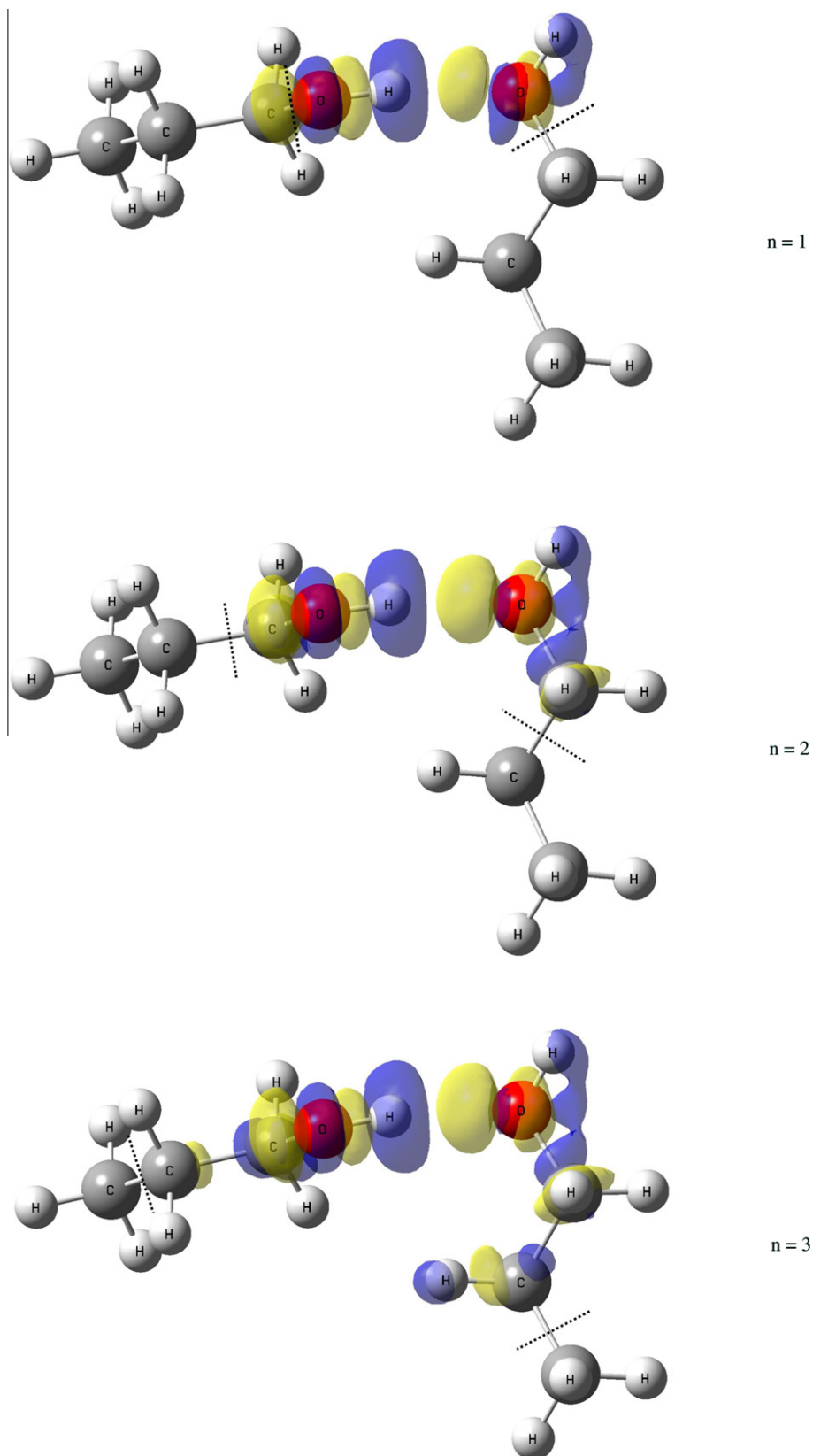


**Fig. 4.** Intramolecular EDS ( $\pm 0.001$  a.u. isosurfaces) for the dimer of propanol at aug-cc-pVTZ level using the fragmentation scheme presented here. The fragmentation order (first, second, and third order) is indicated in the right side of the figures. Blue and yellow regions correspond to negative and positive values of the electron density respectively. The bond broken in each fragmentation order is indicated.

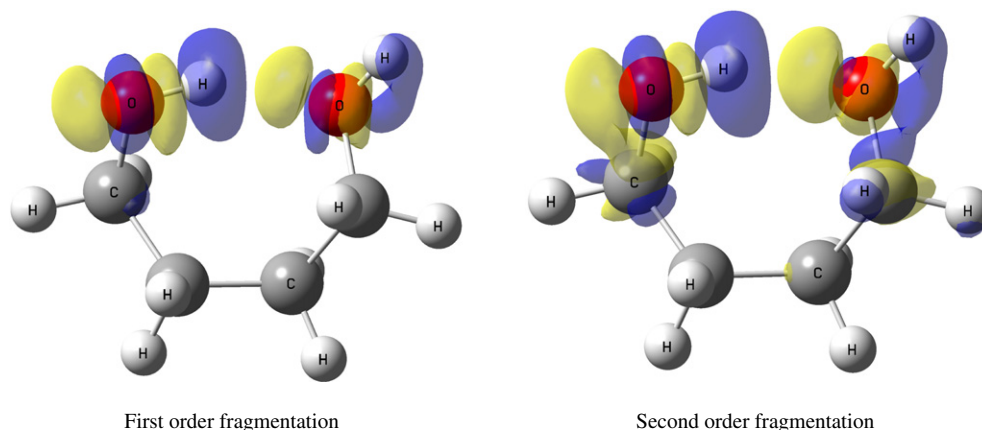


**Fig. 5.** Intramolecular electron density shift ( $\pm 0.001$  a.u. isosurfaces) for 1,4-butanediol at MP2/aug'-cc-pVTZ computational level. Blue and yellow colors correspond to negative and positive values of the electron density, respectively.

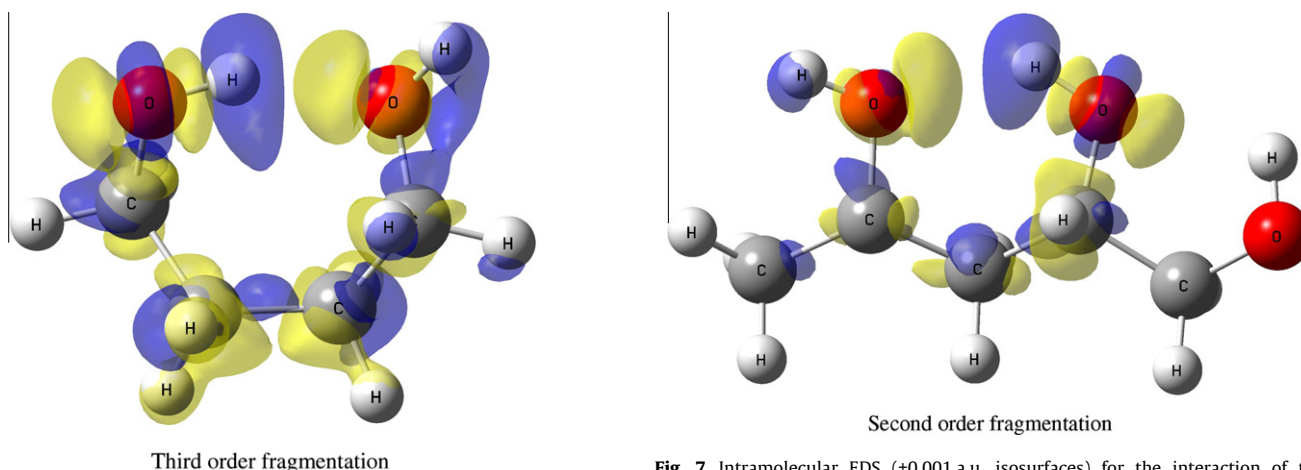


**Fig. 6.** Intramolecular electron density shift ( $\pm 0.001$  a.u. isosurfaces) at third order fragmentation for 1,4-butanediol at MP2/aug'-cc-pVTZ computational level. Blue and yellow regions correspond to negative and positive values of the electron density respectively.

electron density of the C2–C3 bond is not properly compensated with the fragments obtained. Thus, it is observed a non-realistic loss of the electron density in the C2–C3 bonding region while a gain in the surroundings of the hydrogen atoms.

We have also analyzed the charge density shift in between the fragments and the complete molecule. We have performed the basin integration of the atoms within fragments AH and HB and in the AB molecule obtaining the charge associated to each atom. The H of the OH group (hydrogen bond donor) shows a loss of charge (+0.575 to +0.620 a.u.) as it was suggested for intermolecular hydrogen bonds by Koch and Popelier [54].

#### 4.2.2. Case 2: 1,2,4-pentanetriol

The next molecule considered, 1,2,4-pentanetriol, corresponds to a larger system which incorporates multiple HBs. This molecule was previously studied by Deshmukh [31], where the molecular tailoring approach was used to evaluate the intramolecular hydrogen bonds of such molecule. In the present work, the structure has been optimized at MP2/aug'-cc-pVTZ level and afterward an AIM analysis has been performed, finding a BCP between the OH located in C2 and C4, with a OH distance of 2.003 Å, and a electron density of 0.022 a.u. The absence of the OH...O BCP between the hydroxyl groups in C1 and C2 was reported by Klein [55], and discussed by Deshmukh [31].

**Fig. 7.** Intramolecular EDS ( $\pm 0.001$  a.u. isosurfaces) for the interaction of the hydroxyl groups in positions 2 and 4 of 1,2,4-pentanetriol calculated at MP2/aug'-cc-pVTZ computational level. Blue and yellow regions correspond to negative and positive values of the electron density, respectively.

The representation of the EDS for the interaction of the hydroxyl groups in positions 2 and 4 of the 1,2,4-pentanetriol is shown in Fig. 7, with  $\pm 0.001$  a.u. isosurfaces. Note that the region where the OH...O BCP is located presents similar features than those found in the 1,4-butanediol, the electron density shift description of both systems being basically the same. This means that the intramolecular EDS tool may isolate properly the interaction zone of electron density from the entire molecule giving a clear description of it.

The analysis of the EDS due to the interaction between the hydroxyl groups in positions 1 and 2 is shown in Fig. 8. The disposition of these two hydroxyl groups presents an OHO angle of 111.3° which makes the HB interaction unfavorable and thus no BCP is found connecting them. However, a similar pattern of the EDS to those previously found in hydrogen bonds that present BCP is observed but in this case the region with gain/loss of electron density are smaller than in the interaction of the hydroxyl groups in the positions 2 and 4.

#### 4.2.3. Case 3: 4-chlorobutan-1-ol

The 4-chlorobutan-1-ol molecule has been chosen in order to show the results of the intramolecular hydrogen bond between two different moieties. This system presents an OH...Cl interaction characterized by a BCP with an electron density value of 0.021 a.u. and Cl...H distance of 2.301 Å. In Fig. 9 the intramolecular EDS for

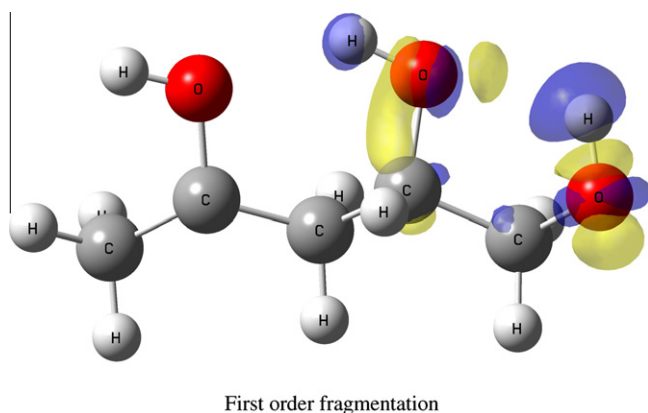


**Fig. 8.** Intramolecular EDS ( $\pm 0.001$  a.u. isosurfaces) for the interaction of the hydroxyl groups in positions 1 and 2 of 1,2,4-pentanetriol calculated at MP2/aug'-cc-pVTZ computational level. Blue and yellow regions correspond to negative and positive values of the electron density, respectively.

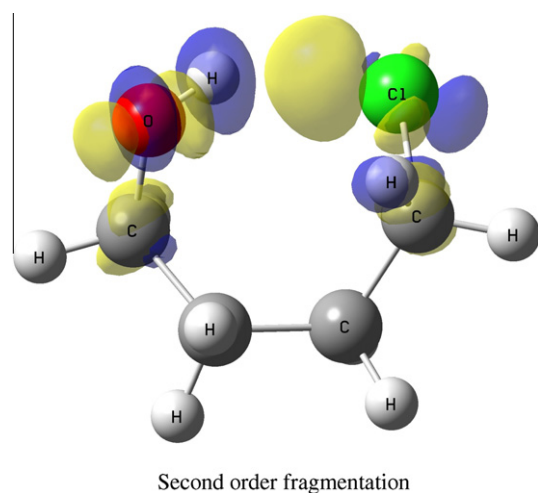


**Fig. 9.** Intramolecular EDS ( $\pm 0.001$  a.u. isosurfaces) for the OH...Cl interaction in 4-chlorobutan-1-ol at MP2/aug'-cc-pVTZ. Blue and yellow regions correspond to negative and positive values of the electron density respectively.

1-chloro-4-butanol with  $\pm 0.001$  a.u. of isosurface values is depicted. The OH...Cl EDS shows an increase of the electron density, as a yellow area, between the H and Cl atoms. This increase is larger than those found in the typical OH...O hydrogen bonds. In this case, the chlorine transfers more density into the yellow area than the O in the 1,4-butanediol. Therefore, the H atom corresponding to the HB donor suffers less negative EDS.

#### 4.2.4. Case 4: 1,8-dihydroxynaphthalene

In cases 4 and 5, 1,8-disubstituted naphthalenes with different groups in positions 1 and 8 (OH, F and CH<sub>3</sub>) have been considered in order to test the suitability of the proposed methodology in aromatic structures. The fragmentation scheme, used here, tries to keep the same logic as the one used for aliphatic chains, but with some warnings. The first order fragmentation consists on an isodesmic reaction without optimization, of the H caps, see Fig. 10. The second order involves the rupture of double C=C bonds. In the method proposed by Deev and Collins [29], the breaking of a double bond was avoided, and the study was restricted to single bond breaks. In the present work, it is observed that the

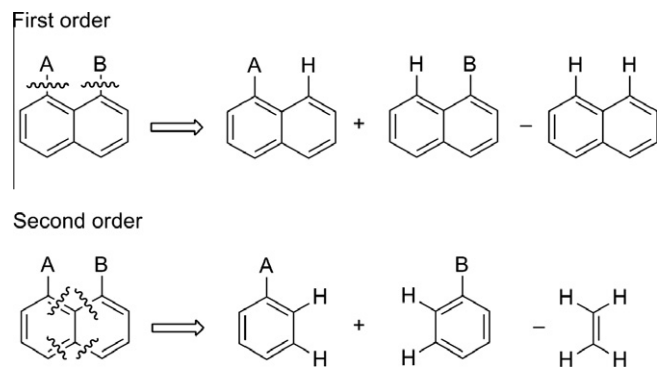


**Fig. 10.** Fragmentation schemes for naphthalene derivatives.

splitting of the molecule involving double bonds in it, leads to a wrong description of the electron density shift.

The naphthalene-1,8-diol system contains exclusively one OH...O interaction, with an interatomic O...H distance of 1.775 Å and a BCP with an electron density value of 0.036 a.u. In Fig. 11, it is shown the EDS for the naphthalene corresponding to the first and second order fragmentation, left and right respectively. At first order, it is observed that the OH...O interaction presents analogous EDS to that calculated for the 1,4-butanediol, with a similar qualitative description of the interaction. In the second order fragmentation it is found a perturbation around the ring which distorts the EDS. Two main effects can explain this. On the one hand, the second order involves the rupture of multiple bond which is one of the limitations of this tool, due to the inefficient description of the C=C electron density. On the other hand, the aromaticity presented in naphthalene is different than the one in the benzene. The molecular partition tries to represent naphthalene using two benzene rings, and therefore, the electron density shift gives very different results due to the notable differences between the two systems [56]. However, the HB interaction mainly retains the picture that we have found for 1,4-butanediol at second order fragmentation. Thus, to obtain a very clean description of the interaction in this type of compounds the first order fragmentation is recommended.

#### 4.2.5. Case 5: F...F and H...H interactions: 1,8-difluoronaphthalene and 1,8-dimethylnaphthalene

The characterization of the F...F interactions in 1,8-difluoronaphthalene (1,8-DFN) and different derivatives was previously studied by Matta et al. [57] These authors considered a 1,8-DFN derivative which presents two methylene groups in 4 and 5 positions, showing H...H interactions. Thus, the 1,8-difluoronaphthalene and 1,8-dimethylnaphthalene molecules have been chosen in order to explore the EDS in systems where some of their moieties could present repulsive interactions. Both present a rigid structure which allows the groups in positions 1 and 8 to be fixed, avoiding changes in the geometry as it will be the case for open carbon chains.

In Fig. 12 is depicted the EDS of the intramolecular interaction of the groups in positions 1 and 8 of 1,8-difluoronaphthalene and 1,8-dimethylnaphthalene. In the case of the difluoro derivative, a region with depletion of electron density between the fluorine appears which corresponds to the repulsion between the two F atoms. The same features can be observed for the methylene derivative where an increase in the electron density around the H atoms and a decrease in the region between the carbon atoms are observed. Those characteristics point to a repulsive interaction between the CH<sub>3</sub> groups.

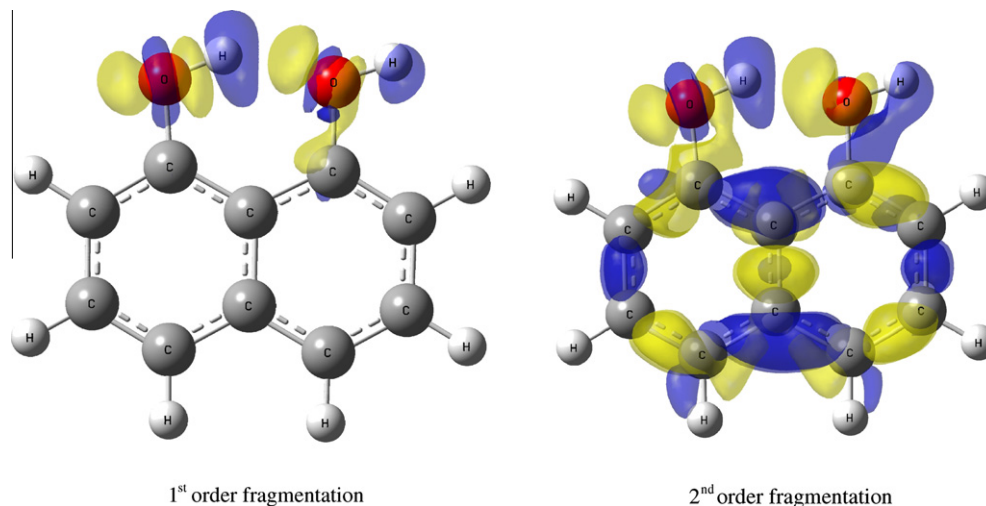


**Fig. 11.** Intramolecular EDS ( $\pm 0.001$  a.u. isosurfaces) for the OH...O interaction in 1,8-naphthalenediol at MP2/aug'-cc-pVTZ computational level. Blue and yellow regions correspond to negative and positive values of the electron density respectively.

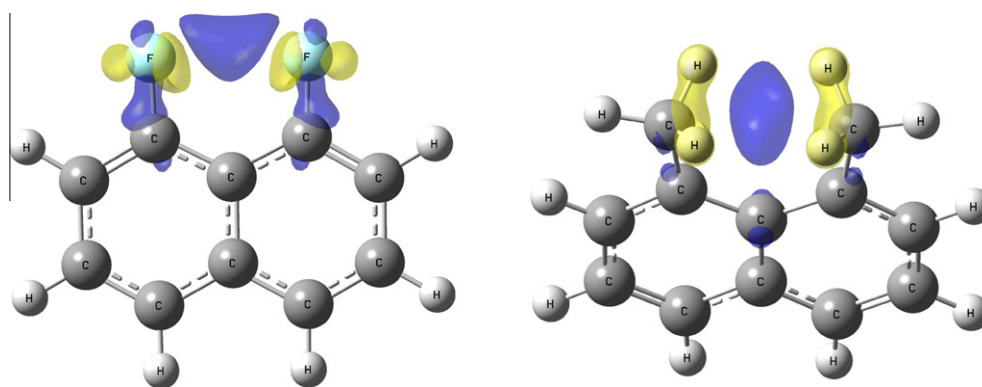


**Fig. 12.** First order intramolecular EDS ( $\pm 0.0005$  a.u. isosurfaces) for the interaction between the groups in positions 1 and 8 of 1,8-difluoronaphthalene (left) and 1,8-dimethylnaphthalene (right) at MP2/aug'-cc-pVTZ computational level. Blue and yellow regions correspond to negative and positive values of the electron density respectively.

#### 4.2.6. Other cases

In this section the intramolecular EDS have been briefly analyzed for a variety of interactions, namely: chalcogen–chalcogen, nitrogen–bromine, nitrogen–boron, dihydrogen, and silicon–nitrogen interactions. It has been summarized the results of these interactions in the present section. The molecules in this section have been selected based on their simplicity and the presence of the interaction of interest.

For chalcogen–chalcogen interactions, we have selected the 1-hydroxy-3-propanetellurol and its fluorine derivate, studied by Minyaev and Minkin [58], which shows a Te...O interaction. The N...Br interaction has been studied using 3-bromocyclohexanamine, a molecule who is a precursor of the metabolite of ketamine [59], and exhibit a N...Br contact. The nitrogen–boron interaction in the 3-borylpropan-1-amine has been chosen in order to show the feasibility of this method dealing with relatively strong interactions. A dihydrogen interaction in the 2-boryl-1-ethanol has been considered in analogy to those systems previously studied by Alkorta et al. [60]. Finally, Si...N interactions have been studied with this technique using two models. The first one is the (*N,N*-dimethylaminoxy)chlorosilane molecule which contains a Si–O–N linkage, from the series of compounds synthesized by Mitzel et al. [61–65] and studied by Murray et al. [66]. The second one, 3-silylpropan-1-amine, considers a carbon backbone.

Fig. 13 shows the EDS for the interaction mentioned above. As general trend, it can be observed the blue and yellow moieties

representing the electron density decrease and increase areas. The donor atom usually presents a yellow area followed by a blue one in between both interacting atoms. In the case of chalcogen interactions (Fig. 13a and b) the donation from the oxygen atom to the Te–H antibond is observed as an increase in the density of the atom attached to the Te, and it is more notable in the fluorine derivate (b) than in the hydrogen substituted (a). In fact, the effect of the F atom within the electron density of the interaction is remarkable comparing Fig. 13a and b.

The N...Br interaction, as it is shown in Fig. 13c, is due to the donation from the lone pair of the N to the Br, being depicted as a yellow area in the N atom and a large blue region between both interacting atoms.

Fig. 13d shows the EDS for the N...B interaction. This interaction is relatively stronger than the previously studied. In order to depict the EDS it has been selected a higher value of the isosurface 0.005 a.u. It can be observed a large yellow region between the N and B atoms, due to the strong interaction which is close to the regimen of a normal bond.

A dihydrogen interaction is studied and depicted in Fig. 13e. It is shown a characteristic yellow region in the H attached to the B atom corresponding to the electron donor atom.

Fig. 13f and g, illustrate both Si...N interactions. Fig. 13f corresponds to a Si...N in with a Si–O–N linkage, and shows the blue region around the N atom due to the electron donations, and a yellow region between the Si and N atoms which represents an

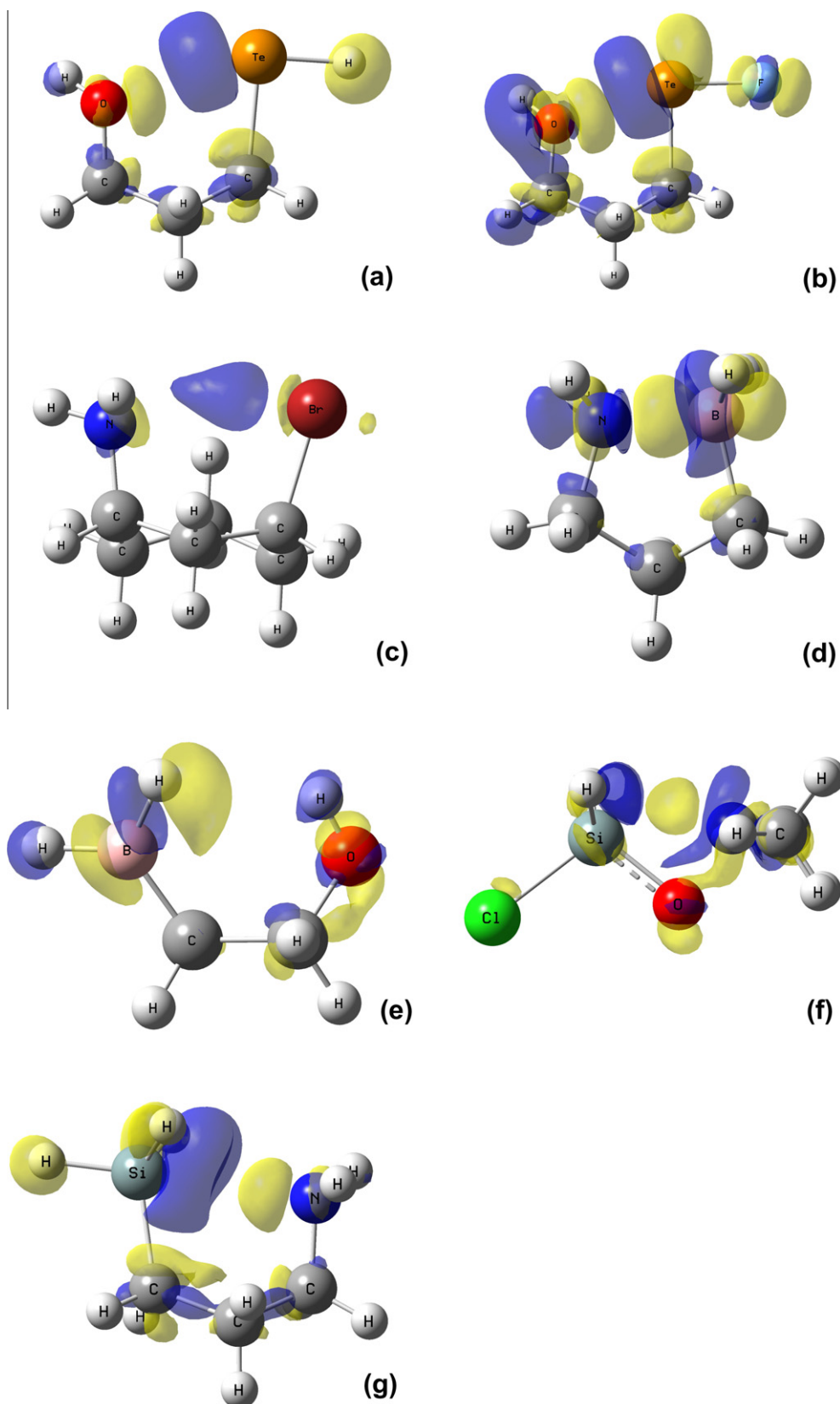


**Fig. 13.** Intramolecular EDS for different cases calculated at MP2/aug'-cc-pVTZ computational level. Blue and yellow regions correspond to negative and positive values of the electron density shift, respectively. (a) 1-hydroxy,3-propanetellurol at second order fragmentation ( $\pm 0.001$  a.u. isosurfaces), (b) 1-hydroxypropyl hypofluortelluroite at second order fragmentation and ( $\pm 0.001$  a.u. isosurfaces), (c) 3-bromocyclohexanamine at first order fragmentation ( $\pm 0.001$  a.u. isosurfaces), (d) borylpropan-1-amine at second order fragmentation ( $\pm 0.005$  a.u. isosurfaces), (e) 3-boryletan-1-ol first order fragmentation ( $\pm 0.0005$  a.u. isosurfaces), (f) (N,N-dimethylaminoxy)chlorosilane at first order fragmentation ( $\pm 0.002$  a.u. isosurfaces), (g) 3-silylpropan-1-amine at first order fragmentation ( $\pm 0.002$  a.u. isosurfaces).

increase in the electron density due to the Si···N interaction. In Fig. 13g, the interaction Si···N shows similar pattern than in the 13f, but the blue region on the N atom is not observed at this iso-surface value of 0.01 (but 0.005). This is because in Fig. 13f the CH<sub>3</sub> groups donate charge to the N, meanwhile in Fig. 13g the H atoms are poor electron donors.

## 5. Conclusions

A new methodology for the study of the EDS in intramolecular interaction based on the molecular fragmentation scheme is described. The methodology has been tested in an intermolecular HB dimer, where the EDS can be obtained as the difference between the complex and the isolated monomer. The Hodgkin similarity index has been used to quantify the similarity between the exact EDS and those obtained by the methodology proposed here. The intramolecular EDS have been calculated for a variety of intramolecular interactions: hydrogen bonds, chalcogen–chalcogen, N···Br, B···N, dihydrogen and Si···N interactions, and also repulsive halogen–halogen and hydrogen–hydrogen contacts, providing a qualitative description in all the cases. Based on this study the following rules for the fragmentation scheme are recommended: (1) select the highest order of fragmentation possible, (2) do not chose that order in which the HH<sup>n</sup> fragment corresponds to the H<sub>2</sub> molecule, (3) only fragmentations which involve the rupture of single bond are allowed.

## Acknowledgments

This work was supported by the Ministerio de Ciencia e Innovación (Project No. CTQ2009-13129-C02-02) and Comunidad Autónoma de Madrid (Project MADRISOLAR2, Ref. S2009/PPQ-1533). The authors thank the CTI (CSIC) and the Centro de Computación Científica at Universidad Autónoma de Madrid for allocation of computer time.

## References

- [1] Y. Maréchan, *The Hydrogen Bond and Water Molecule: The Physics and Chemistry of Water, Aqueous, and Bio-media*, Elsevier, Amsterdam, 2007.
- [2] I.V. Stiopkin, C. Weeraman, P.A. Pieniazek, F.Y. Shalhout, J.L. Skinner, A.V. Benderskii, Hydrogen bonding at the water surface revealed by isotopic dilution spectroscopy, *Nature* 474 (2011) 192–195.
- [3] R.A. Nicodemus, S.A. Corcelli, J.L. Skinner, A. Tokmakoff, Collective hydrogen bond reorganization in water studied with temperature-dependent ultrafast infrared spectroscopy, *J. Phys. Chem. B* 115 (2011) 5604–5616.
- [4] A. Zeidler, P.S. Salmon, H.E. Fischer, J.C. Neufeind, J.M. Simonson, H. Lemmel, H. Rauch, T.E. Markland, Oxygen as a site specific probe of the structure of water and oxide materials, *Phys. Rev. Lett.* 107 (2011) 145501.
- [5] C.F. Matta, N. Castillo, R.J. Boyd, Extended weak bonding interactions in DNA:  $\pi$ -stacking (base–base), base–backbone, and backbone–backbone interactions, *J. Phys. Chem. B* 110 (2005) 563–578.
- [6] H. Khesbak, O. Savchuk, S. Tsushima, K. Fahmy, The role of water H-bond imbalances in B-DNA substrate transitions and peptide recognition revealed by time-resolved FTIR spectroscopy, *J. Am. Chem. Soc.* 133 (2011) 5834–5842.
- [7] E. Yang, S.-Y. Chen, Z.-S. Liu, J.-Q. Li, Unprecedented pseudo water tapes stabilized by a one-dimensional Cu(II) coordination polymer, *Chin. J. Struct. Chem.* 30 (2011) 101–104.
- [8] S. Scheiner, *Hydrogen Bonding. A Theoretical Perspective*, Oxford University Press, Oxford, 1997.
- [9] G.R. Desiraju, T. Steiner, *The Weak Hydrogen Bond*, Oxford University Press, Oxford, 1999.
- [10] S.J. Grabowski, *Hydrogen bonding: new insights*, in: *Challenges and Advances in Computational Chemistry and Physics*, Oxford University Press, Oxford, 2006.
- [11] P. Metrangola, G. Resnati, *Halogen Bonding: Fundamentals and Applications*, Springer, Berlin, 2008.
- [12] M.E. Ali, P.M. Oppeneer, Influence of noncovalent cation/anion– $\pi$  interactions on the magnetic exchange phenomenon, *J. Phys. Chem. Lett.* 2 (2011) 939–943.
- [13] F. Blanco, B. Kelly, I. Alkorta, I. Rozas, J. Elguero, Cation– $\pi$  interactions: complexes of guanidinium and simple aromatic systems, *Chem. Phys. Lett.* 511 (2011) 129–134.
- [14] S. Zahn, R. Frank, E. Hey-Hawkins, B. Kirchner, Pnictogen bonds: a new molecular linker?, *Chem. Eur. J.* 17 (2011) 6034–6038.
- [15] J.E. Del Bene, I. Alkorta, G. Sánchez-Sanz, J. Elguero, 31P–31P spin–spin coupling constants for pnictogen homodimers, *Chem. Phys. Lett.* 512 (2011) 184–187.
- [16] P. Sanz, M. Yáñez, O. Mó, Resonance-assisted intramolecular chalcogen–chalcogen interactions?, *Chem. Eur. J.* 9 (2003) 4548–4555.
- [17] G. Sánchez-Sanz, I. Alkorta, J. Elguero, A theoretical study of the conformation of 2,2'-bifuran, 2,2'-bithiophene, 2,2'-bitellurophene and mixed derivatives: chalcogen–chalcogen interactions or dipole–dipole effects?, *Comput. Theor. Chem.* 974 (2011) 37–42.
- [18] J.W.G. Bloom, S.E. Wheeler, Taking the aromaticity out of aromatic interactions, *Angew. Chem. Int. Ed.* 50 (2011) 7847–7849.
- [19] S.E. Wheeler, Local nature of substituent effects in stacking interactions, *J. Am. Chem. Soc.* 133 (2011) 10262–10274.
- [20] A.S. Jaiilov, S.F. Nelsen, I.A. Guzei, Q. Wu, Intramolecular  $\pi$ -stacking interactions of bridged bis-p-phenylenediamine radical cations and diradical dications: charge-transfer versus spin-coupling, *Angew. Chem. Int. Ed.* 50 (2011) 6860–6863.
- [21] J.-M. Lehn, Toward complex matter: supramolecular chemistry and self-organization, *Proc. Natl. Acad. Sci.* 99 (2002) 4763–4768.
- [22] G.R. Desiraju, Supramolecular synthesis in crystal engineering – a new organic synthesis, *Angew. Chem. Int. Ed.* 34 (1995) 2311–2327.
- [23] A. Milet, T. Korona, R. Moszynski, E. Kochanski, Anisotropic intermolecular interactions in van der Waals and hydrogen-bonded complexes: what can we get from density functional calculations?, *J. Chem. Phys.* 111 (1999) 7727–7735.
- [24] H.L. Williams, C.F. Chabalowski, Using Kohn–Sham orbitals in symmetry-adapted perturbation theory to investigate intermolecular interactions, *J. Phys. Chem. A* 105 (2000) 646–659.
- [25] E.R. Johnson, S. Keinan, P. Mori-Sanchez, J. Contreras-Garcia, A.J. Cohen, W. Yang, Revealing noncovalent interactions, *J. Am. Chem. Soc.* 132 (2010) 6498–6506.
- [26] B. Kuhn, P. Mohr, M. Stahl, Intramolecular hydrogen bonding in medicinal chemistry, *J. Med. Chem.* 53 (2010) 2601–2611.
- [27] E. Espinosa, I. Alkorta, J. Elguero, E. Molins, From weak to strong interactions: a comprehensive analysis of the topological and energetic properties of the electron density distribution involving X–H[centered ellipsis]F–Y systems, *J. Chem. Phys.* 117 (2002) 5529–5542.
- [28] P.R. Mallinson, G.T. Smith, C.C. Wilson, E. Grech, K. Wozniak, From weak interactions to covalent bonds: a continuum in the complexes of 1,8-bis(dimethylamino)naphthalene, *J. Am. Chem. Soc.* 125 (2003) 4259–4270.
- [29] V. Deev, M.A. Collins, Approximate ab initio energies by systematic molecular fragmentation, *J. Chem. Phys.* 122 (2005) 154102–154112.
- [30] D.W. Zhang, J.Z.H. Zhang, Molecular fractionation with conjugate caps for full quantum mechanical calculation of protein–molecule interaction energy, *J. Chem. Phys.* 119 (2003) 3599–3605.
- [31] M.M. Deshmukh, S.R. Gadre, L.J. Bartolotti, Estimation of intramolecular hydrogen bond energy via molecular tailoring approach, *J. Phys. Chem. A* 110 (2006) 12519–12523.
- [32] M.M. Deshmukh, S.R. Gadre, L.J. Bartolotti, Estimation of intramolecular hydrogen bond energy via molecular tailoring approach, *J. Phys. Chem. A* 111 (2007) 10885.
- [33] M.M. Deshmukh, S.R. Gadre, Estimation of N–H···O=C intramolecular hydrogen bond energy in polypeptides, *J. Phys. Chem. A* 113 (2009) 7927–7932.
- [34] R.F.W. Bader, *Atoms in Molecules: A Quantum Theory*, Clarendon Press, Oxford, 1990.
- [35] B. Silvi, A. Savin, Classification of chemical bonds based on topological analysis of electron localization functions, *Nature* 371 (1994) 683–686.
- [36] A.D. Becke, K.E. Edgecombe, A simple measure of electron localization in atomic and molecular systems, *J. Chem. Phys.* 92 (1990) 5397–5403.
- [37] D. Stalke, Meaningful structural descriptors from charge density, *Chem. Eur. J.* 17 (2011) 9264–9278.
- [38] V. Kolman, R. Marek, Z. Strelcova, P. Kulhanek, M. Necas, J. Svec, V. Sindelar, Electron density shift in imidazolium derivatives upon complexation with cucurbit[6]uril, *Chem. Eur. J.* 15 (2009) 6926–6931.
- [39] M. Solimannejad, S.G. Shirazi, S. Scheiner, Analysis of complexes pairing hydroperoxyl radical with peroxyformic acid, *J. Phys. Chem. A* 111 (2007) 10717–10721.
- [40] I. Alkorta, I. Soteras, J. Elguero, J.E. Del Bene, The boron–boron single bond in diborane(4) as a non-classical electron donor for hydrogen bonding, *Phys. Chem. Chem. Phys.* 13 (2011) 14026–14032.
- [41] J.E. Del Bene, I. Alkorta, J. Elguero, Ab initio study of ternary complexes X:(HCNH)<sup>+</sup>:Z with X, Z = NCH, CNH, FH, ClH, and FCl: diminutive cooperative effects on structures, binding energies, and spin–spin coupling constants across hydrogen bonds, *J. Phys. Chem. A* 115 (2011) 12677–12687.
- [42] J.E. Del Bene, I. Alkorta, G. Sánchez-Sanz, J. Elguero, Structures, Energies, bonding, and NMR properties of pnictogen complexes H2XP:NXH2 (X = H, CH3, NH2, OH, F, Cl), *J. Phys. Chem. A* 115 (2011) 13724–13731.
- [43] X.-F. Dong, F.-D. Ren, D.-L. Cao, W.-N. Wang, F.-Q. Zhang, A MP2(full) theoretical investigation on the  $\pi$ -halogen interaction between OCBCO and X1X2 (X1, X2 = F, Cl, Br), *J. Mol. Struct. THEOCHEM* 961 (2010) 73–82.
- [44] M. Solimannejad, M. Malekani, I. Alkorta, Cooperative and diminutive unusual weak bonding in F3CX···HMgH···Y and F3CX···Y···HMgH Trimers (X = Cl, Br; Y = HCN, and HNC), *J. Phys. Chem. A* 114 (2010) 12106–12111.

- [45] S. Scheiner, U. Adhikari, Abilities of different electron donors (D) to engage in a P...D noncovalent interaction, *J. Phys. Chem. A* 115 (2011) 11101–11110.
- [46] S. Scheiner, Effects of substituents upon the P...N noncovalent interaction: the limits of its strength, *J. Phys. Chem. A* 115 (2011) 11202–11209.
- [47] C. Møller, M.S. Plesset, Note on an approximation treatment for many-electron systems, *Phys. Rev.* 46 (1934) 618–622.
- [48] D.E. Woon, T.H. Dunning, Gaussian basis sets for use in correlated molecular calculations. V. Core-valence basis sets for boron through neon, *J. Chem. Phys.* 103 (1995) 4572–4585.
- [49] T.H. Dunning, Gaussian-Basis sets for use in correlated molecular calculations. I. The atoms boron through neon and hydrogen, *J. Chem. Phys.* 90 (1989) 1007–1023.
- [50] M.J. Frisch, G.W. Trucks, H.B. Schlegel, G.E. Scuseria, M.A. Robb, J.R. Cheeseman, G. Scalmani, V. Barone, B. Mennucci, G.A. Petersson, H. Nakatsuji, M. Caricato, X. Li, H.P. Hratchian, A.F. Izmaylov, J. Bloino, G. Zheng, J.L. Sonnenberg, M. Hada, M. Ehara, K. Toyota, R. Fukuda, J. Hasegawa, M. Ishida, T. Nakajima, Y. Honda, O. Kitao, H. Nakai, T. Vreven, J. Montgomery, J. A., J.E. Peralta, F. Ogliaro, M. Bearpark, J.J. Heyd, E. Brothers, K.N. Kudin, V.N. Staroverov, R. Kobayashi, J. Normand, K. Raghavachari, A. Rendell, J.C. Burant, S.S. Iyengar, J. Tomasi, M. Cossi, N. Rega, N.J. Millam, M. Klene, J.E. Knox, J.B. Cross, V. Bakken, C. Adamo, J. Jaramillo, R. Gomperts, R.E. Stratmann, O. Yazyev, A.J. Austin, R. Cammi, C. Pomelli, J.W. Ochterski, R.L. Martin, K. Morokuma, V.G. Zakrzewski, G.A. Voth, P. Salvador, J.J. Dannenberg, S. Dapprich, A.D. Daniels, Ö. Farkas, J.B. Foresman, J.V. Ortiz, J. Cioslowski, D.J. Fox, Gaussian 09, Gaussian, Inc., Wallingford CT, 2009.
- [51] T.A. Keith, AIMAll, TK Gristmill Software (aim.tkgristmill.com), in, 2011, pp. TK Gristmill Software, (aim.tkgristmill.com).
- [52] E.E. Hodgkin, W.G. Richards, Molecular similarity based on electrostatic potential and electric field, *Int. J. Quant. Chem. Quant. Biol. Symp.* 14 (1987) 105–110.
- [53] A.J.L. Jesus, M.T.S. Rosado, I. Reva, R. Fausto, M.E.S. Eusébio, J.S. Redinha, Structure of isolated 1,4-butanediol: combination of MP2 calculations, NBO analysis, and matrix-isolation infrared spectroscopy, *J. Phys. Chem. A* 112 (2008) 4669–4678.
- [54] U. Koch, P.L.A. Popelier, Characterization of C—H—O hydrogen bonds on the basis of the charge density, *J. Phys. Chem.* 99 (1995) 9747–9754.
- [55] R.A. Klein, Electron density topological analysis of hydrogen bonding in glucopyranose and hydrated glucopyranose, *J. Am. Chem. Soc.* 124 (2002) 13931–13937.
- [56] G. Portella, J. Poater, J.M. Bofill, P. Alemany, M. Solà, Local aromaticity of [n]acenes, [n]phenacenes, and [n]helicenes ( $n = 1-9$ ), *J. Org. Chem.* 70 (2005) 2509–2521.
- [57] C.F. Matta, N. Castillo, R.J. Boyd, Characterization of a closed-shell fluorine–fluorine bonding interaction in aromatic compounds on the basis of the electron density, *J. Phys. Chem. A* 109 (2005) 3669–3681.
- [58] R.M. Minyaev, V.I. Minkin, Theoretical study of O → X (S, Se, Te) coordination in organic compounds, *Can. J. Chem.* 76 (1998) 776–788.
- [59] R.F. Parcell, J.P. Sanchez, Synthesis of ketamine metabolites I and II and some anomalous reactions of 6-bromoketamine, *J. Org. Chem.* 46 (1981) 5055–5060.
- [60] I. Alkorta, J. Elguero, S.J. Grabowski, How to determine whether intramolecular H...H interactions can be classified as dihydrogen bonds, *J. Phys. Chem. A* 112 (2008) 2721–2727.
- [61] N.W. Mitzel, U. Losehand,  $\beta$ -donor bonds in compounds containing SiON fragments, *Angew. Chem. Int. Ed.* 36 (1997) 2807–2809.
- [62] N.W. Mitzel, U. Losehand,  $\beta$ -donor interactions of exceptional strength in *N,N*-dimethylhydroxylaminochlorosilane,  $\text{ClH}_2\text{SiONMe}_2$ , *J. Am. Chem. Soc.* 120 (1998) 7320–7327.
- [63] N.W. Mitzel, U. Losehand, A. Wu, D. Cremer, D.W.H. Rankin, (*N,N*-dimethylaminoxy)trifluorosilane: strong, dipole moment driven changes in the molecular geometry studied by experiment and theory in solid, gas, and solution phases, *J. Am. Chem. Soc.* 122 (2000) 4471–4482.
- [64] N.W. Mitzel, K. Vojinović, R. Fröhlich, T. Foerster, H.E. Robertson, K.B. Borisenko, D.W.H. Rankin, Three-membered ring or open chain molecule –  $(\text{F}_3\text{C})_2\text{SiONMe}_2$ , a model for the  $\alpha$ -effect in silicon chemistry, *J. Am. Chem. Soc.* 127 (2005) 13705–13713.
- [65] N.W. Mitzel, A.J. Blake, D.W.H. Rankin,  $\beta$ -donor bonds in SiON units: an inherent structure – determining property leading to (4+4)-coordination in tetrakis-(*N,N*-dimethylhydroxylamido)silane, *J. Am. Chem. Soc.* 119 (1997) 4143–4148.
- [66] J. Murray, M. Concha, P. Politzer, Molecular surface electrostatic potentials as guides to Si—O—N angle contraction: tunable  $\sigma$ -holes, *J. Mol. Model.* 17 (2011) 2151–2157.